1 Reviewer #1 (R. Gladstone)

The authors present approaches to parameterising grounding line modelling specific to the finite element approach. Such parameterisations have been used in different models, but parameterisations presented here are designed to work in particular with the finite element method. The authors have carried out experiments based on the MISMIP3D experimental design, and demonstrate that a combination of high resolution and parameterisation of the grounding line are necessary for self-consistent model behaviour. This is not a new result in ice sheet modelling in general, as it is broadly consistent with several other studies using different ice sheet models, but it provides new insight specific to marine ice sheet modelling using the finite element method to solve the SSA equations. The paper is, on the whole, clearly written and well supported by the plots. The choice of material relegated to the appendices seems good to me. Of the three parameterisations presented it is disappointing that SEP3 has not been investigated in more detail, and I would strongly urge the authors to carry out some further simulations with SEP 3 at a lower resolution, say 5km, and see how effectively this approach can address the grounding line problem. I know of other researchers in the area who have expressed a strong interest forms of p-refinement, and who would I am sure be very keen to see SEP3 explored further in this paper.

We followed the suggestion of the reviewer and added SEP3 runs for the 5 km resolution meshes, which confirmed our conclusions.

Goldberg 2009 used a very similar model, but with h-refinement and r-refinement. I think the SEP3 approach is perhaps similar to p-refinement? Would it make sense to describe it in such terms or do I misunderstand p-refinement?

In finite elements, h-refinement refers to the size of the elements of the mesh, p-refinement to the order of the polynomial basis functions of the space of solution and r-refinement to the relocation or moving of a mesh. The SEP3 approach is different from p-refinement, as the order of the polynomial basis function remains here the same (P1 Linear Lagrange elements), only the number of integration points is increased.

Please be careful about using the term "lower" with regard to spatial resolution as it can be ambiguous. Please use either "coarser" or "finer" as these terms are not open to ambiguity. E.g. lines 23-24 page 3338

Done

Specifics
Abstract
L9-12. I looked for where you say how your simulations "explain why some

vertically..." but I couldn't find it. At one point in the discussion you seem to suggest it is coincidence. Can you support this statement?

We agree with the reviewer that our manuscript explains why the results from the HSE model in *Pattyn et al.* [2012] are different from the other SSA models and not why they are similar to the Full-Stokes results. This was clarified in the manuscript.

L15-16. Suggest rewording for clarity: "...the reversibility test can be passed at much lower resolutions than are required for convergence of the steady-state grounding line position."

Done

L16. Surely here you mean "fixed grid SSA models" rather than "fixed grid models"? Or are you claiming to have demonstrated that Stokes flow models using a contact condition to determine grounding line position are also inadequate even at very high resolution?

Done

L18-20. The resolution recommendations are specific to this experimental setup and should not be presented as though they are generally applicable to real marine ice sheet systems. The actual resolution will vary with bedrock slope, buttressing, bed slipperiness (see for example Gladstone 2012 Annals Glac. paper). I think you either need to qualify or remove this statement.

Done

Page 3337
Line 18. "model data"? You mean forcing data, or model inputs? It may be difficult, but it HAS been applied to real glaciers, e.g. Favier 2014 for PIG.

We clarified the sentence.

3338
L22-24. Please state where these numbers come from. Note that the resolution requirements will also be a function of bed slipperiness and amount of buttressing (demonstrated in Gladstone et al 2012 Annals of Glaciology paper). There may be important real world systems for which coarser resolutions than 500m are adequate.

Done

3340
L6-7. I think this sentence can lead to confusion when introducing the parameterisations. Perhaps it would be more helpful to the reader (such as myself)

less familiar with finite element methods to say that, since the finite element method is being used and C is nodal, C is allowed to vary linearly (in the case of first order elements) through the element, but in fact C is spatially constant for most of the domain (all of the domain except the elements containing the grounding line in fact, since it is constant for all grounded nodes). I would then re-iterate in the paragraph on page 3341, lines 20-26, that integration is of a linearly varying quantity C. The visual representation in Fig 1 is excellent, but I feel this slight enhancement to the explanation would benefit those unfamiliar with finite elements.

We added clarification and specificities for this set-up in the experiment section.

3342 L27 and 3343 L1 please name the relevant variables. Specifically, refer to C and m in equation 2.

Done

3344.
L5 "models" $\rightarrow$ "simulations"

Done

L7 "runs" $\rightarrow$ "simulations"

Done

L9-11 I think it would be better to define your steady state criteria as part of the experiment design section (section 3). At page 3343 line 11 I think would be good.

We think that this criteria is not really part of the experiment but more a tool to analyze the results so we kept it in the results section.

3345
L9. "estimate" $\rightarrow$ "quantification". This isn't an estimate for the spread, it IS the spread!

Done

L13-16. This should be merged with the figure caption. The caption should be a concise summary for the reader to understand what is shown in the figure. It doesn't need to be repeated in the text. The figure should just be referred to here rather than caption information given.

Done

L10 "models" → "simulations".

Done

L20 "models" → "simulations".

Done

3346
L11-12. This is not true for NSEP 250m, which does show retreat after the advance.

Done

3347
L5-6 what does the phrase "buttressing from basal friction" mean? Do you just mean the resistance to flow due to basal friction? If so this is not buttressing. Or perhaps you mean that where the perturbed basal friction is reduced the relatively higher basal friction in the other part of the domain has a retarding effect on the more slippery region through long stresses, in which case I think a little more explanation than "buttressing from basal friction" would be helpful.

We changed the sentence to "resistance from the basal friction".

L4-6. I am not convinced by this explanation, possibly because I don't fully understand it. I think the key here is the basal friction rather than flux where the model thinks the grounding line is. It is clear from your experiments that if you apply zero basal friction to the first floating element you underestimate grounding line position, whereas if you apply full basal drag over the whole of the first floating element you overestimate grounding line position (ok, you haven't done this exactly, but you can see that SEP 1 and SEP2 are intermediates to these extremes: SEP 1 has higher basal friction than SEP2 and slightly over estimates grounding line position whereas SEP 2 slightly underestimates grounding line position, referring to Figure 2). Basically, the more drag you apply to the element that should contain the grounding line, the more resistance to motion you impose, the thicker your ice gets, and the more your grounding line will tend to advance.

We agree that the critical aspect here is where the basal friction is applied and rephrased the sentence.

3348
L9-10 I think the other Gladstone 2010 paper (in The Cryosphere) has a better analysis of convergence errors, though I don't consider it essential to go further into convergence issues in the current study.

Done

L11 please avoid the term "higher" with regard resolution as it can be ambiguous. Please say "coarser" or "finer".

Done

L12 "verify" → "satisfy" (2 counts)

Done

L14 "exhibits" → "exhibit"

Done

L20-23. Do you think this indicates a weakness in the MISMIP3D experimental design, or a fundamental difference between steady state and transient grounding line behaviour in models?

This is a very good question and I am not sure that we have what we need to address it here; it would require additional experiments with different configurations.

3349

L2 please indicate that you recognise that the suggested 2km resolution requirement is specific to this experimental setup and not generally applicable. See also Gladstone 2012 Annals Glac.

Done

L4-5 is it not true that SEP2 always leads to lower basal friction than SEP1? Because they both use the same area fraction for the grounded portion of the element while calculating basal friction, but SEP 1 uses C over that area whereas SEP2 integrates between C and zero. Is that right? It is my interpretation of SEP1 and SEP2 but doesn't seem to be explicitly discussed in the paper, so maybe I misunderstood?

The friction law used in this experiment depends on the basal friction, which varies within an element. So if the integral of the friction coefficient C is the same for SEP1 and SEP2 in this case (as C is constant over the whole grounded area), the integral of basal friction varies as the velocity varies within an element. This is why we did not mention this point in the paper.

L7-9 Why? For fully grounded elements SEP1 and SEP2 are the same. For elements containing the grounding line SEP2 will always give lower friction than SEP1. So why should there be greater difference between the two with spatially varying basal friction coefficient?

We agree that for fully grounded elements, both SEP1 and SEP2 are the same. For the elements that are crossed by the grounding line, SEP2 have either lower or higher friction than SEP1 depending on the distribution of the friction coefficient within the element, so if the distribution of friction has large variations, we expect the difference to be larger.

3350 final paragraph. This is a very interesting discussion. I don't know of anyone who has yet worked on a SEP for the contact condition in a Stokes Flow model. Could be important for the future. It might also be worth considering that different basal drag parameterisations could lead to easier grounding line migration (e.g. Gunter Leguy 2014 TCD).

We are not aware of any SEP for full-Stokes flow.

3351
General comment on conclusions. Remember that these results were achieved with an SSA finite element model using the MISMIP3D setup, and may be specific to those conditions. I think it reasonable to generalise up to a point, as these results are similar to other studies with different model types. But the conclusions read as though you are presenting new general conclusions. But really you are presenting new conclusions specific to SSA and your FE SEPs, which are consistent with existing results in supporting more general conclusions across model types. I would suggest subtle rewording along these lines.

We rephrase the conclusions following the suggestions of the reviewer.

L17 again the 2km is specific to the setup up. Please qualify this statement or remove it.

Done

Tables and Figures Table 1 and 2: "15" or "fifteen"? I don't mind but be consistent. I think better to say "simulations" than "models". ISSM is the model.

Done

Figure 2. I think you could add SEP 3 to fig 2. Of course you would need an extra x-axis (perhaps place it at the top?) and the axes would not be directly comparable, so maybe you would prefer to place it in a separate subplot. But one way or another I would love to see the convergence of SEP3 plotted.

Results from SEP3 are presented on figure 7. This figure shows the convergence of SEP3 with the order of the integration.

Figure 3. Add to the caption that where the black line is not visible this means it is overlain by the blue line (if that is indeed the case?). Clarify in the caption that the blue line is the new steady state position after the forcing perturbation has been reset.

Done

Figures 3 and 4 should really be one big figure if such a large figure is allowed.

We agree with the reviewer that one big figure would be much better. The format of TCD (landscape paper) did not allow us to do it but it will hopefully be fixed with the TC format (portrait).

Figure 5. Caption. “green” -¿ “blue” or “teal”. Can you please clarify the direction of te time axis: is it reversed for the blue/green lines? In other words, after the perturbation evolution is in the direction from y=100 to y=0? If this isn’t the case then I can’t understand why the blue curves don’t start from the same x values as the final position of the red curves. If it is the case then please make this clear in the caption.

Done

Figures 5 and 6 should really be one big figure if such a large figure is allowed. Figure 7. Blue stars is SEP3? Why not label it as such?

We agree that this would be better as for fig. 3 and 4.

2 Reviewer #2 (F. Pattyn)

General appreciation

This is a timely paper that investigates how numerical models can be improved to capture grounding line migration based on the intercomparison work of MISMIP and MISMIP3d. The participating model HSE1 in the latter intercomparison (Pattyn et al. 2013) did show a behaviour that was not possible to explain at that time, and the work presented by Seroussi et al. gives (i) a clarification on this and - more importantly - some solutions as how to improve its accuracy and performance. Since the MISMIP3d intercomparison other people have investigated the possibility to improve both accuracy and performance. One of these is due to Feldmann et al (2014) - Journal of Glaciology, a paper that not only should be referred to, but also needs closer attention to put the results of Seroussi et al in a wider context, since it is not the first paper that explores grounding line interpolations in planview (vertically integrated) models. At the time of MISMIP3d very few (if not only one) model(s) used grounding line interpolations, which limited conclusions beyond recommendations of grid resolution. The advent of interpolation studies show that alternative techniques may aid at obtaining solutions for coarser resolutions. However, in this sense, and interpolation can be regarded as locally increasing spatial resolution by subdividing a mesh into sub-elements.

We thank the reviewer for suggesting to compare our results with [*Feldmann et al.*, 2014]. This is now included in the new manuscript.

I was quite intruiged by this paper, and more so by its promises. The abstract clearly mentions that "Our simulations explain why some vertically depth-averaged model simulations exhibited behaviors similar to full-Stokes models in the MISMIP3D benchmark". However I did not find any clarification beyond the fact that we are dealing with a numerical artifact. Moreover, it fortifies my belief that this is pure coincidence.

We agree that the agreement of the grounding line position with the full-Stokes models is probably a coincidence even though our results suggest that it might be linked to the absence of sub-element parameterizations in full-Stokes models, but this should be further investigated before any conclusions can be drawn. We clarified the text to remove this ambiguity.

This brings me to another point that is stated in the abstract: "The results reveal that differences between simulations performed with and without sub-element parameterization are as large as those performed with different approximations of the stress balance equations and that the reversibility test can be passed at much lower resolutions than the steady-state grounding line position." This statement argues that numerical noise is of the order of magnitude as the effect of stress approximations and that the difference can only be reduced by making use of sub-element parameterization. Here we need to make a clear difference between approximating a physical process and the way it is numerically approximated. Both are two different types of approximations: the goal of a numerical model is to be free of numerical bias and to demonstrate that the physical model (represented by full Stokes or any of the approximations to this system) is accurately represented/captured. This was the focus of the Pattyn and Durand paper (2013): by only selecting models that were free of numerical biases, i.e., that not only showed reversibility but also took the finest spatial resolution computationally possible resulting in smooth grounding lines (void of numerical noise - see the selection criteria in the Supplementary Material of that paper), it was clear that a distinction between physical approximations could easily be made. Therefore it was possible to investigate what the impact of physics is on grounding line migration. So, it is not only a question of spatial resolution, it is also question of having a stable numerical solution.

This is a very good point. However, we show here that all grounding line parameterizations do converge as we refine the mesh, but the final positions of the grounding lines are different. It is therefore not a problem of numerical noise or stable implementation. All the parameterizations presented in this paper are stable and the steady-state grounding line converges towards an infinitely refined grounding position at fine mesh resolution. However this converged grounding line position varies depending on the sub-grid parameterization chosen, leading to very large differences, comparable to the spread of results obtained with different approximations of the stress balance solutions. The question of sub-grid parameterization is still open for full-Stokes models in particular, as no sub-grid parameterization exists today and we do not know the impact it has on model simulations.

In this respect, the authors should reformulate their abstract/discussion/conclusions

and make numerical noise reduction their ultimate goal. The reversibility test is only a parameter amongst so many that helps at improving our understanding of grounding line migration. It should be clear that "passing the reversibility test" does not make your model correct. Furthermore, the conclusions should be put in the light of "this particular experimental setup". Since other setups are not tested, we don't know whether the slightly convex grounding lines are representative of capturing grounding lines in Antarctica (nevertheless, Favier et al (2014) have shown that model numerics did have a minor effect compared to model physics in their simulation of Pine Isalnd Glacier with three different approximations to the Stokes equations). One should remain very careful.

We rephrased the discussion and conclusions to clarify that reversibility is only one of the possible tests and that our onclusions are based only on one particular set-up. However, as mentioned above, using sub-grid parameterization is not just a problem of noise reduction, and is actually very relevant to full-Stokes models, as no sub-grid parameterization exists today for this case.

Detailed remarks

Page 3341: "... in the reset of the manuscript": remainder of the manuscript.

Done

Page 3343, last line: I wouldn't state "usually associated with". Only the

MISMIP papers put spatial resolution forward as a solution due to the lack of other measures. You could be precise and specifically mention that those papers demonstrate that increase in spatial resolution improved the accuracy of the solution.

Done

Page 3344: Results section, first sentence: add ", respectively" at the end of

this sentence

Done

Page 3350: line 17-20: this is only valid for this particular setup of the experiment and cannot be generalized.

Done

Figures 3 and 4: make coloured lines thicker

Done

3 Short comment #1 (A. Levermann)

Perhaps our paper Feldmann et al. Resolution-dependent performance of grounding line motion in a shallow model compared to a full-Stokes model according to the MISMIP3d intercomparison Journal of Glaciology 60 (220) (2014), 353-360, doi:10.3189/2014JoG13J093. would be of interest for this study. Cheers, Anders

Done

4 Short comment #2 (G. Durand)

"We expect our results to be similar for higher-order (HO) models". This would be, to my opinion, very valuable to demonstrate this assertion. This all the more important, that the authors usually do not use an SSA model but the Batter-Pattyn for simulation of actual glaciers (e.g. http://www.the-cryosphere-discuss.net/8/1873/2014/tcd-8-1873- 2014-discussion.html).

We tried to run a couple experiments with a higher-order (HO) model to strengthen our conclusions and demonstrate the accuracy of the HO model. However these runs are computationally intensive if we want to start with a 1 m thick ice and not bias the model with the initial conditions. We were able to run a few simulations at 5 km resolution. Results are similar to SSA with a steady-state grounding line located at 213.8 km, 613.4 km and 503.9 km respectively for NSEP, SEP1 and SEP2. This is respectively 26 km downstream, 18 km upstream and 45 km upstream of the corresponding SSA models. Reversibility was achieved for the both SEP1 and SEP2 (see figure below in the case of SEP1). It is however impossible to extrapolate these results and difficult to draw some strong conclusions using simulations performed at 5 km mesh resolution only.

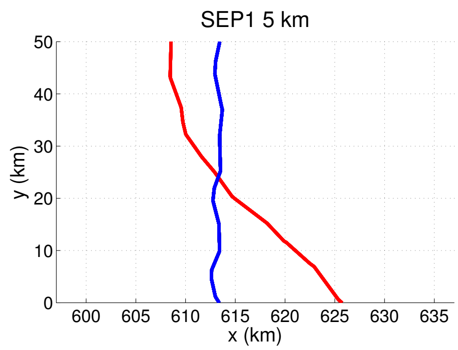
SEP1 5 km
y (km)
x (km)
0
10
20
30
40
50
600
605
610
615
620
625
630
635

References

Feldmann, J., T. Albrecht, C. Khroulev, P. F., and A. Levermann, Resolution-dependent performance of grounding line motion in a shallow model compared with a full-Stokes model according to the MISMIP3d intercomparison, *J. Glaciol.*, *60*(220), 353–359, doi:10.3189/2014JoG13J093, 2014.

Pattyn, F., et al., Results of the Marine Ice Sheet Model Intercomparison Project, MISMIP, *The Cryosphere*, *6*(3), 573–588, doi:10.5194/tc-6-573-2012, 2012.

Manuscript prepared for The Cryosphere Discuss.
with version 3.5 of the LaTeX class copernicus_discussions.cls.
Date: 2 October 2014

Hydrostatic grounding line parameterization in ice sheet models

H. Seroussi[1] , M. Morlighem[2] , E. Larour[1] , E. Rignot[2,1], and A. Khazendar[1]

[1]Jet Propulsion Laboratory - California Institute of Technology, 4800 Oak Grove Drive MS 300-323, Pasadena, CA 91109-8099, USA
[2]University of California, Irvine, Department of Earth System Science, Croul Hall, Irvine, CA 92697-3100, USA

Correspondence to: Helene Seroussi (Helene.Seroussi@jpl.nasa.gov)

Abstract

Modeling of grounding line migration is essential to simulate accurately the behavior of marine ice sheets and investigate their stability. Here, we assess the sensitivity of numerical models to the parameterization of the grounding line position. We run the MISMIP3D benchmark experiments using a two-dimensional shelfy-stream approximation (SSA) model with different mesh resolutions and different sub-element parameterizations of grounding line position. Results show that different grounding line parameterizations lead to different steady state grounding line positions as well as different retreat/advance rates. Our simulations explain why some vertically depth-averaged model simulations ~~exhibited behaviors similar to full-Stokes models in the MISMIP3D benchmark, while the~~ deviate significantly from the vast majority of simulations based on SSA ~~showed results deviating significantly from full-Stokes results~~in the MISMIP3D benchmark. The results reveal that differences between simulations performed with and without sub-element parameterization are as large as those performed with different approximations of the stress balance equations ~~and~~ in this configuration. They also demonstrate that the reversibility test ~~can be passed at much lower resolutions than~~ is passed at relatively coarse resolution while much finer resolutions are needed to accurately capture the steady-state grounding line position. We conclude that fixed grid SSA models that do not employ such a parameterization should be avoided, as they do not provide accurate estimates of grounding line dynamics, even at high spatial resolution. For models that include sub-element grounding line parameterization, in the MISMIP3D configuration, a mesh resolution ~~lower~~ finer than 2 km should be employed.

1 Introduction

Mapping of grounding lines, where ice detaches from the underlying bedrock and becomes afloat in the ocean, is possible using satellite remote sensing with either visible imagery (Bohlander and Scambos, 2007) or differential radar interferometry (Goldstein et al., 1993; Rignot et al., 2011b). Observations show that grounding lines have a dynamic behavior. This is particularly the case in the Amundsen Sea sector of West Antarctica, where their migration inland reaches more than 1 km/yr on Pine Island and Thwaites Glacier (Rignot et al., 2011a). Accurate knowledge of grounding line positions as well as their evolution in time is therefore critical to understand ice sheet dynamics. Grounding lines are indeed a fundamental control of marine ice sheet stability (van der Veen, 1985; Hindmarsh and Le Meur, 2001), and they also determine the shape of ice-shelf cavities, which affect ocean-induced melting rates (Schodlok et al., 2012). Grounding line dynamics are strongly non-linear, with long episodes of relative stability interrupted by significant retreat, this evolution being controlled, among other factors, by basal topography (Weertman, 1974; Durand et al., 2009b). The Antarctic ice sheet is surrounded by floating ice shelves of varying size, and modeling of this transition zone is therefore essential to simulate the evolution of polar ice sheets in our changing climate.

However, accurate modeling of this transition zone remains both a scientific and technical challenge. Three-dimensional (3D) full-Stokes (FS) models are required in order to fully resolve the contact problem between the ice and the underlying bedrock (Nowicki and Wingham, 2008; Durand et al., 2009b,a; Favier et al., 2014). This approach ~~has been applied to synthetic geometries and~~ is computationally intensive and sensitive to model data, so it ~~is difficult to apply~~ has been applied to synthetic geometries mainly and starts to be applied for real glaciers (Favier et al., 2014). Alternative approaches that have been widely used rely on the hydrostatic criterion to estimate the grounding line position: ice shelves are assumed to float hydrostatically in ocean water (Huybrechts, 1990; van der Veen, 1985; Ritz et al., 2001). Models often rely on fixed grids or meshes for which each grid cell or element is either entirely floating or entirely grounded. This method limits the precision of the grounding line position and simulations show a strong dependency on grid size. A fine mesh resolution is then required in the grounding zone in order to accurately capture grounding line migration and reduce numerical artifacts caused by model discretization (Vieli and Payne, 2005; Katz and Worster, 2010). Using sub-grid parameterization, which tracks the grounding line position within the element, improves models based on hydrostatic equilibrium condition and reduces their dependency on grid size (Pattyn et al., 2006; Gladstone et al., 2010a; Winkelmann et al., 2011). Another alternative is to use moving grid or adaptive mesh refinement, so that the mesh or grid resolution follows the grounding line transition zone (Goldberg et al., 2009; Cornford et al., 2013). These methods overcome the difficulties associated to grounding line discretization but lead to more complicated frameworks and remain difficult to implement in parallelized architectures. Due to the high computational time associated with fine resolution meshes or grids, most studies investigating the impact of grounding line parameterization, mesh resolution or stress balance approximation are performed on one-dimensional (1D) flowline or two-dimensional (2D) flow-band models (e.g., Vieli and Payne (2005); Pattyn et al. (2006); Schoof (2007a,b); Katz and Worster (2010); Gladstone et al. (2010a); Pattyn et al. (2012)). They show the strong dependency of model results on mesh resolution in the grounding line transition zone. They also demonstrate that moving grid models explicitly tracking grounding line position are able to reduce the dependency of results on mesh resolution. Analyses on 2D planview or 3D models confirm these results (Goldberg et al., 2009; Cornford et al., 2013). Recent results using planview shallow models and finite differences (Feldmann et al., 2014) also show that including grounding line sub-grid parameterization in shallow models allows to capture grounding line reversibility at low resolutions without including a flux correction.

Benchmark efforts, such as the Marine Ice Sheet Model Intercomparison Project (MISMIP), that compare results from a variety of ice flow models and spatial resolutions, have been performed for both flow line (MISMIP) and planview (MISMIP3D) models. They compare the sensitivity of modeled grounding line migration to numerical implementation (Pattyn et al., 2012, 2013; Pattyn and Durand, 2013). Results indicate that planview models need to include at least membrane stress components to be able to capture the grounding line position and that this position depends on the degree of sophistication of the model. Results also emphasize the need to use spatial resolution ~~lower~~ finer than 500 m when relying on fixed grid discretization and ~~lower~~ finer than 5 km when sub-grid parameterizations are included in the MISMIP3D configurations (Pattyn et al., 2013).

These conclusions are however drawn from a variety of models based on different softwares and different approximations for the stress balance equations, with different grounding line parameterizations, using either structured or unstructured meshes that are either fixed or adapted with time. It is therefore difficult to attribute the differences of the model results to either the approximation made in the stress balance equations or to the parameterization adopted to capture the grounding line position. In the MISMIP3D experiments for example, some results based on the shelfy-stream approximation (SSA, MacAyeal, 1989) ~~are comparable to results produced with FS, while most SSA models exhibit a significantly different behavior~~deviate significantly from the vast majority of SSA model results. The differences in the grounding line positions between models based on the SSA are either due to differences in grounding line parameterization or domain discretization.

In this study we assess the impact of different sub-element parameterizations for hydrostatic grounding line treatment using a single ice flow model. Experiments are based on the MISMIP3D configurations. We use the Ice Sheet System Model (ISSM, Larour et al. (2012)) to solve the 2D shelfy-stream equations with spatial resolutions varying between 5 km and 250 m. We analyze the grounding line steady state position, its evolution following a perturbation in basal friction and the reversibility of its evolution for the different grounding line parameterizations. We conclude on the requirements needed to accurately capture grounding line motion and the impact of the underlying parameterization.

2 Model

2.1 Field equations

The 2D SSA (SSA, MacAyeal, 1989) is employed for both grounded and floating ice, so membrane stress terms are included but all vertical shearing is neglected. Ice viscosity, μ, is considered to be isotropic and to follow Glen's flow law (Cuffey and Paterson, 2010):

$$\mu = \frac{B}{2\dot{\epsilon_e}^{\frac{n-1}{n}}} \tag{1}$$

where B is the ice hardness, $\dot{\epsilon_e}$ the effective strain rate and $n = 3$ Glen's exponent.

A non-linear friction law that links basal shear stress to basal sliding velocity is applied on grounded ice:

$$\boldsymbol{\tau}_b = C|\boldsymbol{u_b}|^{m-1}\boldsymbol{u_b} \tag{2}$$

where $\boldsymbol{\tau}_b$ is the basal shear stress, $\boldsymbol{u_b}$ the basal sliding velocity, C the friction coefficient and m the sliding law exponent. C is ~~a nodal value~~ defined on each node and the friction coefficient therefore varies linearly within an element. Thickness evolution is dictated by mass conservation.

The position of the grounding line is determined by a floatation criterion: ice is floating if its thickness, H, is equal or lower than the floating height H_f defined as:

$$H_f = -\frac{\rho_w}{\rho_i} r,\ r < 0 \tag{3}$$

where ρ_i is the ice density, ρ_w the ocean density and r the bedrock elevation (negative if below sea level). Grounding line is therefore located where $H = H_f$:

$$H > H_f \quad \text{ice is grounded} \tag{4}$$

$$H = H_f \quad \text{grounding line position} \tag{5}$$

$$H < H_f \quad \text{ice is floating} \tag{6}$$

2.2 Domain discretization

The domain is discretized with a 2D isotropic uniform unstructured triangle mesh. Velocity and geometry fields are computed on each vertex of the mesh using Lagrange P1 (piecewise linear) finite elements. Element size varies between 5 km for the lowest resolution and 250 m for the highest resolution and is uniform within each mesh.

Grounding line position (Fig. 1a) is based on the hydrostatic equilibrium condition as described above and three different techniques are used to parameterize its position. As the same SSA equations are used on the entire domain to compute the stress balance, the only difference between grounded and floating ice is the presence or absence of basal friction.

In the first method, each element of the mesh is either grounded or floating: floatation criterion is determined on each vertex of the triangle and if at least one vertex of the triangle is floating, the element is considered floating and no friction is applied. Otherwise, if the three vertices are grounded, the element is considered grounded. This is the simplest approach used by fixed grid models to determine grounding line positions (Vieli and Payne, 2005), in which the grounding line is defined as the last grounded point. We refer to this technique as no sub-element parameterization (NSEP, Fig. 1b).

In the second method, the floating condition is a 2D field and the grounding line position is determined by the line where $H = H_f$, so it is located anywhere within an element. Some elements are therefore partly grounded and partly floating. In this case the initial basal friction C is reduced to match the amount of grounded ice in the element as proposed by Pattyn et al. (2006) and Gladstone et al. (2010a) but for a 2D element:

$$C_g = C\,\frac{A_g}{A} \tag{7}$$

where C_g is the applied basal friction coefficient for the element partially grounded, A_g is the area of grounded ice of this element and A is the total area of the element. As all fields and data are computed using piecewise linear function, the grounding line position within each triangle is a straight line. This technique is referred to as sub-element parameterization 1 (SEP1, Fig. 1c) in the remainder of the paper.

In the third method, the grounding line position is located anywhere within an element as for SEP1, but the basal friction computed for partly grounded elements differs. We take advantage of finite element properties to integrate the basal friction only on the part of the element that is grounded. This can be done simply by changing the integration area from the initial element to the grounded part of the element, over which the basal friction is unchanged. This technique is referred to as sub-element parameterization 2 (SEP2, Fig. 1d) in the ~~rest~~ remainder of the manuscript.

In the fourth method, the sub-element parameterization is based on the number of integration points. We test the performance of this method by looking at the steady-state grounding line position (see experiments description below) for a spatial resolution of 1km. The finite element method consists of calculating integrals over each element using a given set of integration points, also called Gaussian quadrature (Zienkiewicz and Taylor, 1989). The number of integration points in each element depends on the degree of polynomial functions being integrated, with more integration points required for polynomial functions of higher degree. In our case, the basal friction goes from zero on the floating part of the element to the value specified in the experiment section, so this step function would require an infinite number of integration points to be exact. An alternative to the two SEP described above is to increase the number of integration points in the integrals and include basal friction for integration points whose thickness is higher than the floating height. SEP3 only allows a finite number of grounding line positions to be captured within the element contrary to the other two SEP. We tested this alternative solution on the 1 km mesh, with integration orders going from 2 to 20, which is equivalent to a number of integration points varying between 3 and 79. This technique is referred to as sub-element parameterization 3 (SEP3, Fig. 1e).

Appendix A details the different descriptions of the stiffness matrix associated to basal friction for all the sub-element parameterizations.

3 Experiments

We reproduce the MISMIP3D setup (Pattyn et al., 2013) and run similar experiments to investigate the influence of spatial resolution and grounding line parameterization on grounding line position and migration. Ice flows over a bedrock with a constant downward sloping bed that varies only in the x direction. The bedrock elevation is defined as:

$$b(x,y) = -100 - x \tag{8}$$

Ice hardness, B, is uniform over the whole domain and equal to 2.15×10^8 Pa s$^{-1/3}$; the basal friction coefficient, C, is also uniform for all grounded ice and equal to 10^7 Pa m$^{-1/3}$ s$^{1/3}$, so on C is constant over each element except for those containing the grounding line, where it varies linearly; the friction law exponent, m is equal to 1/3. The domain is rectangular and stretches between 0 and 800 km in the x direction and 0 and 50 km in the y direction. The boundary conditions applied are as follows: a symmetric ice divide is considered at $x=0$ so the velocity is equal to zero. Water pressure is applied at $x=800$ km to model contact with the ocean. There is a symmetry axis at $y=0$ that represents the centerline of the ice stream and a free slip condition for $y=50$ km, so there is no flux advected through these surfaces and the tangential velocity is equal to zero.

Starting from a thin layer of ice of 10 m, a constant accumulation $\dot{a}$ of 0.5 m yr^{-1} is applied over the whole domain. The marine ice sheet evolves until a steady state configuration is reached. At each time step, we compute the ice velocity, its thickness, the new grounding line position and update the upper and lower surfaces.

This steady state configuration is then perturbed by changing the basal friction coefficient C. This parameter is adjusted spatially using a Gaussian bump such that:

$$C^{\star}=C\left[1-0.75\exp\left(-\frac{(x-x_b)^2}{2x_c^2}-\frac{(y-y_b)^2}{2y_c^2}\right)\right] \tag{9}$$

with $C^{\star}$ the new friction coefficient, x_b the grounding line position at $y=0$ km in the steady state configuration, $y_b=0$, $x_c=150$ km and $y_c=10$ km the spatial extent of the perturbation along the x and y directions. The model is run forward in time for 100 years. The sliding friction is then reset to its initial uniform value and the model runs forward in time until a new steady state configuration is reached. This experiment is designed to assess the ability of models to provide reversible grounding line positions under simplified conditions (Pattyn et al., 2013). The marine ice sheet theory states that ice resting on a down sloping bed without lateral variations exhibits only one steady state grounding line position (Schoof, 2007b). ~~Failure~~ MISMIP benchmark demonstrated that failure to reproduce the reversibility test is ~~usually~~ often associated with coarse mesh resolution.

Steady state and reduced friction experiments are run with five different meshes, with spatial resolution ranging from 5 km to 250 m, for a number of elements varying between ~~2,553~~ 2553 and 1~~,~~013~~,~~894 depending on the spatial resolution. The first three grounding line parameterizations (NSEP, SEP1 and SEP2) are run for all mesh resolutions, resulting in a total of 15 ~~models.~~ simulations. The last grounding line parameterization (SEP3) is only run to find the initial steady state grounding line position for meshes of 5 km and 1 km resolution, with a varying number of integration points (19 simulations).

4 Results

We consider that steady state is reached when the rate of change in ice thickness, grounding line position and ice velocity are all respectively lower than 10^{-5} m/yr , 10^{-3} m/yr and 10^{-5} m/yr^2, respectively. It takes approximately 50,000 years to reach steady state. We need to ensure the Courant-Friedrichs-Lewy condition (CFL, Courant et al., 1967) for all models, so meshes with finer resolution require smaller time steps than the ones with coarser resolution. The initial grounding line position for each of the 15 models is summarized in table 1. It varies between $x = 188$ km and $x = 632$ km depending on the model resolution and grounding line parameterization. In the case of NSEP, the grounding position varies by several hundreds of kilometers (between 188 km and 558 km), while SEP1 and SEP2 lead to variations in steady state grounding line positions of 50 km or less (between 605 km and 632 km and between 550 km and 603 km respectively for the SEP1 and SEP2). This spread in grounding line positions is much larger than in Feldmann et al. (2014); however they start with a slightly different configuration with 500 m thick ice and a grounding line already located around 325 km. Steady state grounding line positions at $y = 0$ km for all parameterizations and mesh resolutions are shown on Fig. 2. Grounding line is moving upstream as the mesh resolution increases for SEP1, while it is moving downstream for NSEP and SEP2. Steady-state grounding line ~~position~~ positions found with SEP3 ~~at 1 km resolution is~~ are in good agreement with SEP2 ~~as it varies between~~ for both 5 km and 1 km mesh resolutions. It varies between $x = 540$ and $x = 497$ km, and $x = 584$ and $x = 589$ km for mesh resolutions of 5 and 1 km, depending on the integration order (see 7), which is ~~within~~ respectively within 10 km and 3 km of SEP2 for a similar resolution when using enough integration points.

As for the domain configuration, the model parameterization and forcings do not vary in the y direction and we have $u_y(x,0) = u_y(x,50) = 0$, the grounding line position should therefore be a straight line parallel to the y axis. In practice, this position slightly varies with y, especially since we use an unstructured mesh. We define the grounding line span as:

$$\Delta GL = \max(x_{gi}) - \min(x_{gi}) \tag{10}$$

where x_{gi} are all grounding line positions for $0 < y < 50$ km. The grounding line span is presented in table 1 and provides ~~an estimate~~ a quantification of the spread of grounding line positions. ΔGL is about twice the size of the elements for NSEP and less than half this size for SEP1 and SEP2.

The perturbation experiment is performed to analyze the reversibility of the grounding line position in a simplified configuration. Fig. 4 shows ~~results of this experiment: the initial steady state grounding line position (black line), its position 100 years after the basal perturbation is introduced (red line) and the new steady state position after the basal friction is reset to its initial value (blue line). The grounding line~~ that grounding line advances along the glacier centerline as the basal friction is reduced in this area, and retreats along the free slip boundary. Advance and retreat extents vary depending on grounding line parameterizations and mesh resolutions. Distances of advance along the centerline and retreat along the free-slip boundary after 100 years for all 15 ~~models~~ simulations are presented in table 2. Advances are more pronounced and retreats are reduced at low resolutions, except for SEP1 that exhibits similar advance and retreat for all mesh sizes. Both SEP1 and SEP2 present advance and retreat after 100 years that converged toward 10 km and 6.5 km respectively at high resolution.

The updated steady state position reached after the perturbation experiment is identical to the initial steady state position (Fig. 4), except for NSEP simulations at low resolution (more than 1 km resolution), so most ~~models~~ simulations exhibit reversibility. The difference between the initial and final grounding line position is less than 10 meters in all the cases where the two steady state grounding line positions superimpose on Fig. 4.

To analyze the motion of the grounding line during the perturbation experiment, Fig. 6 presents the 100 year advance and first 100 year retreat of the grounding line position during the basal perturbation experiment for the different resolutions and grounding line parameterizations. Migration of grounding line position for $y = 0$ and $y = 50$ km is shown (one value every year). For NSEP (first column), grounding line position advances and retreats in discrete steps that are linked to the element size. For both SEP1 and SEP2 (second and third columns), the advance and retreat are continuous. Grounding line advance at $y = 50$ km takes between 20 and 40 years to reach its most advanced position. In the case of NSEP, the grounding position remains stable after the advance, while for SEP1~~and~~, SEP2 and NSEP at 250 m resolution, it is followed by a small retreat. Grounding line retreat at $y = 0$ km takes longer than the advance at $y = 50$ km and is still evolving after 100 years in most cases, which shows that the grounding line is still far from having reached a new steady state position.

5 Discussion

In this study, we investigate the influence of grounding line parameterization on grounding line steady state position as well as its dynamic response to a perturbation in basal friction in the grounding line area. The three grounding line parameterizations all show a dependence on mesh resolution as well as convergence of the grounding line steady state position with ~~higher~~ finer mesh resolution. Convergence of grounding line steady state position is achieved within a few kilometers for SEP1 and SEP2, while it has not fully converged for NSEP. Even at 250 m resolution, grounding line position using NSEP is located several tens of kilometers upstream of SEP1 and SEP2 grounding line position. This behavior is also observed for the HSE model in Pattyn et al. (2013) that was also relying on ISSM and did not include sub-element parameterization of grounding line position. The mesh resolution of this model around the grounding line was 200 m and the grounding line steady state position is located at 545 km, which is about 50 km upstream of the other SSA models and consistent with the results presented here. Indeed, in the case of NSEP, the grounding line is located at the last grounded point. ~~Ice at~~ Basal friction downstream of this point is ~~thicker than above the exact hydrostatic grounding line position, so the ice flux over the grounding line is overestimated, buttressing~~ set to zero so the resistance from basal friction is reduced, and ice flows faster. This leads to a thinner ice sheet and a simulated grounding line position upstream of the one computed with models that include sub-element parameterization. It is a coincidence that this position is similar to models that include vertical shear, which reduces the effective ice viscosity and also results in faster flow and grounding line position farther upstream (Pattyn et al., 2013). Results of the FPA2 model, also performed with an SSA model, NSEP and the same 200 m resolution shows a similar behavior to a smaller extent, with a grounding line position located around 580 km.

The results presented here show that proper grounding line parameterization is crucial for marine ice sheet simulations as discrepancies of several tens of kilometers exist between the different parameterizations and sub-element parameterization should be included. The steady state grounding line positions using SEP1 and SEP2 are consistent with models presented in Pattyn et al. (2013). Differences between simulations carried out with and without SEP are as large as those performed with different stress balance approximations in Pattyn et al. (2013), demonstrating the critical impact of SEP. For example at 500 m resolution, the steady-state grounding line position varies between 522 km and 605 km for NSEP and SEP1 respectively, so more than 80 km. In Pattyn et al. (2013), the same grounding line position computed with FS and hybrid L1L2 models (Hindmarsh, 2004) varies by less than 10 km, and by up to 80 km between FS and SSA models.

Some previous results on flowband models (Gladstone et al., 2010a) exhibit unstable behavior in grounding line retreat in the case of NSEP. We did not experience this kind of behavior and all simulations were stable and converged to a steady state position. Grounding line advance and retreat was also continuous and located anywhere within the element, with no sign of preferred position within the element as observed in Gladstone et al. (2010a) when using SEP1 and SEP2. The second horizontal dimension of our model and the unstructured nature of our mesh may explain these differences.

As expected, grounding line span, ΔGL, is higher than model resolution for the NSEP while it is less than half of the model resolution for SEP1 and SEP2 (see table 1). Differences in grounding line position between models based on a 500 m and 250 m mesh resolution is respectively 25 km, 0.5 km and 3.2 km for NSEP, SEP1 and SEP2. This suggests that grounding line position has not converged for NSEP, while the convergence error is 0.5 km and 3.2 km respectively for the SEP1 and SEP2, as defined in Gladstone et al. (2010a,b).

In the reversibility test, all models except NSEP at a resolution equal or higher than 1 km

~~verify~~ satisfy the reversibility condition. Numerical requirement to ~~verify~~ satisfy the reversibility criterion is therefore a resolution below 1 km for NSEP; whereas all models based on sub-element parameterization ~~exhibits~~ exhibit reversibility even when relying on a coarse mesh. These ~~requirements are less strict than those mentioned in , which might be explained by the very strict conditions imposed to reach the steady state, that resulted in longer initializations (more than 50,000 years)~~results are consistent with Feldmann et al. (2014): reversibility is observed for grid resolutions lower than 2 km for NSEP and with grid resolutions as low as 16 km when SEP is applied. The reversibility criterion is a however necessary condition that provides insights in the numerical aspects of the marine ice sheet model and the simulations, but this test can be passed at relatively low resolutions for which steady-state grounding line positions are not accurate. It therefore does not guarantee the accuracy of the numerical treatment of the grounding line and sufficient mesh resolution, as suggested by the large number of our simulations that verify the reversibility with different steady state grounding line positions.

If we compare SEP1 and SEP2, Fig. 2 shows that they both converge towards the same position for fine mesh resolutions, but that positions at ~~lower~~ coarser resolutions are upstream of the “converged” position for SEP1, and downstream for SEP2. The dynamic advance is also slightly different: grounding line advance at $y = 0$ km is faster and goes farther for the SEP1. It is also associated to a larger retrograde retreat in the second part of the experiment, which is especially pronounced at low resolutions. The grounding line retreat at $y = 50$ km is also larger for SEP1 at low resolution, but both exhibit similar behaviors for resolutions ~~lower~~ finer than 2 km. A mesh resolution ~~lower~~ finer than 2 km should therefore be employed to accurately capture dynamic behavior or marine ice sheet in this configuration. SEP2 is a more “exact” solution, as basal friction is integrated over the exact grounded part of the element, while SEP1 uses an area scaling of the basal friction. In this experiment, the basal friction is uniform over the whole domain, so it is not surprising that SEP1 and SEP2 lead to similar results. We expect greater differences to appear in the case where basal friction varies over the domain, but this is beyond the scope of this paper.

SEP3 was tested only to find the steady-state position of the grounding line on the 5 km and 1 km ~~mesh~~meshes. This method only allows a finite number of grounding line positions to be captured within the element contrary to the other two SEP. We tested this solution on the 5 km and 1 km ~~mesh~~meshes, with integration orders going from 2 to 20. Results on Fig. 7 show that increasing the number of gauss points ~~does not have a big~~ only have an impact on grounding line position ~~:~~ for coarse mesh resolutions. For the 1 km mesh, integration with order of 4 or below leads to one position, and integration with order of 5 and above leads to a second position~~. However~~; however, the grounding line position is within 3 km of the SEP2. For the 5 km mesh, the spread in grounding line positions is much larger, with steady-state grounding line positions varying by more than 50 km. If the integration order is greater than 12, however, these positions is located within 10 km of the SEP2 position. Increasing the number of integration points is therefore a simple solution to include basal friction in a portion of the element in a finite element framework, and provides results similar to other sub-element parameterizations if the integration order is sufficient. This method should be further investigated using ~~different~~ a larger range of mesh resolutions to ensure convergence of the grounding line position at finer mesh resolutions.

The results presented in this paper were all performed using a 2D SSA model and unstructured uniform isotropic meshes. Refinement away from the grounding line is important to accurately capture shear margins (Raymond, 1996) or topography that varies over short distances, but should not be uniform and be based, for example, on the Hessian of the velocity (Morlighem et al., 2010). Increasing mesh resolution has a double impact on computational time. First, increasing the number of degrees of freedom increases computational time, mainly when solving the linear systems. Second, as the elements are smaller, the time steps allowed in transient simulations in order to fulfill the CFL condition are reduced. Fine mesh resolution is therefore necessary in critical areas but alternatives less computationally intensive should also be explored. Adding grounding line parameterizations is a simple improvement as grounding line positions are better captured at no additional cost. Sub-element parameterization allows grounding line position to be anywhere within an element, but the shape of the grounding line is still constrained by the mesh resolution: exact grounding line position within an element remains a straight line if piecewise linear elements are used. Mesh refinement and parameterizations are therefore two methods that should be combined.

This study shows that different grounding line parameterizations lead to different grounding line steady state positions as well as different dynamic behaviors. Differences in model simulations performed with and without SEP are as large as differences between models relying on different ice flow approximations in the MISMIP3D results (Pattyn et al., 2013), which demonstrate the importance of grounding line parameterization. We expect our results to be similar for higher-order (HO) models (Blatter, 1995; Pattyn, 2003). This is because HO models are similar to SSA (HO models include vertical shear stress as well), and the grounding line position is based on the hydrostatic condition in both cases. Models that do not include sub-element parameterizations will need a significantly finer mesh resolution to converge, and the grounding line position may likely be located further upstream than those based on a sub-element parameterization. Recent studies show that relying on full-Stokes in some critical areas in the model domain is necessary (Hindmarsh, 2004; Gudmundsson, 2008; Morlighem et al., 2010), and that grounding line position is better resolved using a contact mechanics condition in this case (Nowicki and Wingham, 2008; Durand et al., 2009b). This condition, however, is only evaluated on the edge or face on which the stress tensor is computed, and no SEP has yet been formulated for such models. This may explain why a very fine resolution on the order of tens of meters must be employed to model grounding line dynamics with FS in some cases (Durand et al., 2009b)~~, and not doing this may also be the reason why steady state grounding line positions of these models are located tens of kilometers upstream relative to the SEP approach~~.

6 Conclusions

In this study, we used a two-dimensional shelfy-stream approximation with fixed unstructured meshes of varying resolution and the MISMIP3D set-up to investigate the impact of several grounding line parameterizations on grounding line dynamics. We show that mesh refinement and grounding line parameterization both have a significant influence on modeled grounding line positions, as well as advance and retreat rates. Models that do not use sub-element parameterizations of grounding line position exhibit a steady state grounding line position located at least several tens of kilometers further upstream than those computed with sub-element parameterizations, even at a high spatial resolution of 250 m. Differences between simulations performed with and without sub-element parameterization are as large as those performed with different approximations of the stress balance in this configuration and the reversibility criterion is satisfied at a much ~~lower~~ coarser resolution that the one required to reach convergence for the steady-state grounding line position. We therefore do not recommend using fixed mesh models that do not rely on sub-element parameterization unless sensitivity to mesh resolution is thoroughly tested. All the sub-element parameterizations tested converged towards the same results at high resolution, and we suggest that mesh refinement in grounding line areas should remain below about two kilometer, as results with different sub-parameterizations are all similar at these resolutions in the simulations presented here.

Appendix A Description of basal friction integration

We detail here the stiffness matrices associated to basal friction on grounded ice for the different sub-element parameterizations. Let $\mathcal{V}$ be the space of kinematically admissible velocity fields and $\mathbf{\Phi} = (\phi_x, \phi_y) \in \mathcal{V}$ a kinematically admissible velocity field. For any $\mathbf{\Phi} \in \mathcal{V}$ the stiffness matrix in the case of NSEP is:

$$K_f = \int_{\Gamma_g} C \boldsymbol{u_b} \cdot \mathbf{\Phi} d\Gamma \tag{A1}$$

where Γ_b is the lower surface of the ice sheet where ice is grounded.

Using a decomposition over the elements and using integration points to calculate the integral gives:

$$K_f = \sum_{E_g} \sum_{g} C \boldsymbol{u_b}(g) \cdot \mathbf{\Phi}(g) W_g \tag{A2}$$

where E_g are the grounded element, g the integration points used for the integration and W_g the weight associated to each integration point.

For SEP1, the friction coefficient is affected by the grounded area of each element, so the stiffness matrix is:

$$K_f = \sum_{E_g} \sum_{g} C_g \boldsymbol{u_b}(g) \cdot \boldsymbol{\Phi}(g) W_g \tag{A3}$$

where C_g is the applied basal friction coefficient for elements partially grounded ($C_g = C$ for elements completely grounded).

For SEP2, the friction is applies only on the grounded part of the element, so the domain of integration is changed to $\tilde{E}_g$ instead of E_g:

$$K_f = \sum_{\tilde{E}_g} \sum_{g} C \boldsymbol{u_b}(g) \cdot \boldsymbol{\Phi}(g) W_g \tag{A4}$$

where $\tilde{E}_g$ corresponds exactly to the brown area on fig.1d. In the code, this is done creating sub-regions within each element partly grounded by determining the exact location of the points where $H = H_f$ and changing the integration domain over these sub-regions.

For SEP3, the stiffness matrix is changed to:

$$K_f = \sum_{E_g} \sum_{g} C \delta(g) \boldsymbol{u_b}(g) \cdot \boldsymbol{\Phi}(g) W_g \tag{A5}$$

where $\delta(g)$ is evaluated at each integration point:

$$\delta(g) = \begin{cases} 1 \text{ if } H > H_f \\ 0 \text{ if } H \leq H_f \end{cases} \tag{A6}$$

Acknowledgements. H.S. was supported by an appointment to the NASA Postdoctoral Program at the Jet Propulsion Laboratory, administered by Oak Ridge Associated Universities through a contract with NASA. This work was performed at the Jet Propulsion Laboratory, California Institute of Technology, and at the Department of Earth System Science, University of California Irvine. A.K. and M.M. were supported by grants from the National Aeronautics and Space Administration's Cryospheric Sciences

Program. E.L. was supported by grants from NASA's Cryospheric Sciences and Modeling, Analysis and Prediction Programs. We thank R. Gladstone, F. Pattyn, G. Durand and A. Levermann for their suggestions which improve the quality of the manuscript.

Table 1. Initial grounding line position and span for the 15 ~~models~~simulations.

GL Parameterization	Resolution	GL($y = 0$ km)	GL($y = 50$ km)	ΔGL
NSEP	5 km	187.5 km	188.4 km	5,009 m
NSEP	2 km	406.3 km	407.6 km	3,439 m
NSEP	1 km	481.2 km	480.3 km	2,000 m
NSEP	500 m	522.7 km	522.2 km	879 m
NSEP	250 m	558.4 km	558.2 km	440 m
SEP1	5 km	631.7 km	631.9 km	782 m
SEP1	2 km	609.8 km	610.2 km	670 m
SEP1	1 km	604.9 km	604.8 km	292 m
SEP1	500 m	605.0 km	605.0 km	148 m
SEP1	250 m	605.5 km	605.6 km	108 m
SEP2	5 km	550.3 km	551,1 km	1215 m
SEP2	2 km	575.0 km	574.8 km	429 m
SEP2	1 km	592.2 km	591.9 km	381 m
SEP2	500 m	599.1 km	599.1 km	170 m
SEP2	250 m	603.3 km	603.4 km	126 m

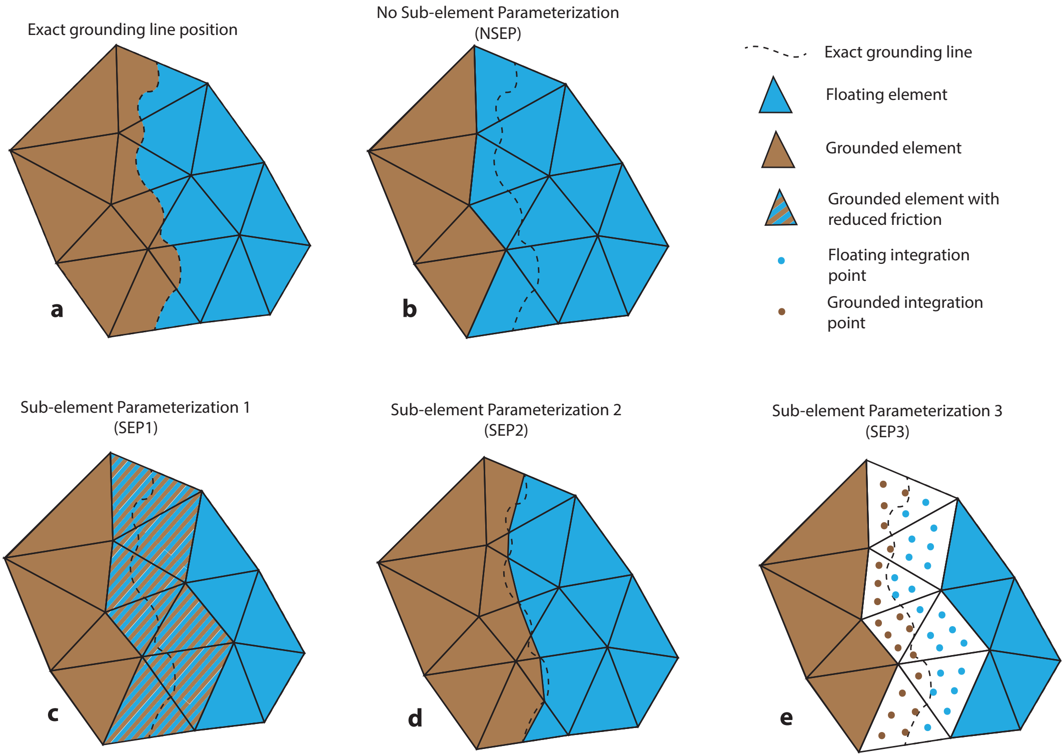

Fig. 1. Grounding line discretization. Grounding line exact location (a), no sub-element parameterization (NSEP, b), sub-element parameterization 1 (SEP1, c), sub-element parameterization 3 (SEP2, d) and sub-element parameterization 3 (SEP3,e).

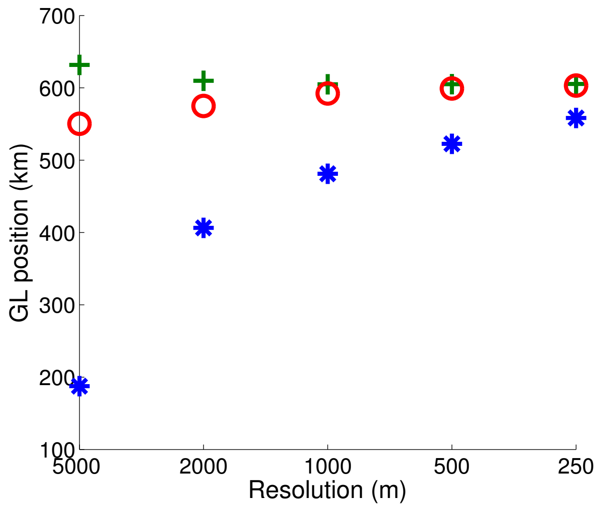

Fig. 2. Steady state grounding line position in $y = 0$ as a function of mesh refinement for NSEP (blue stars), SEP1 (green crosses) and SEP2 (red circles).

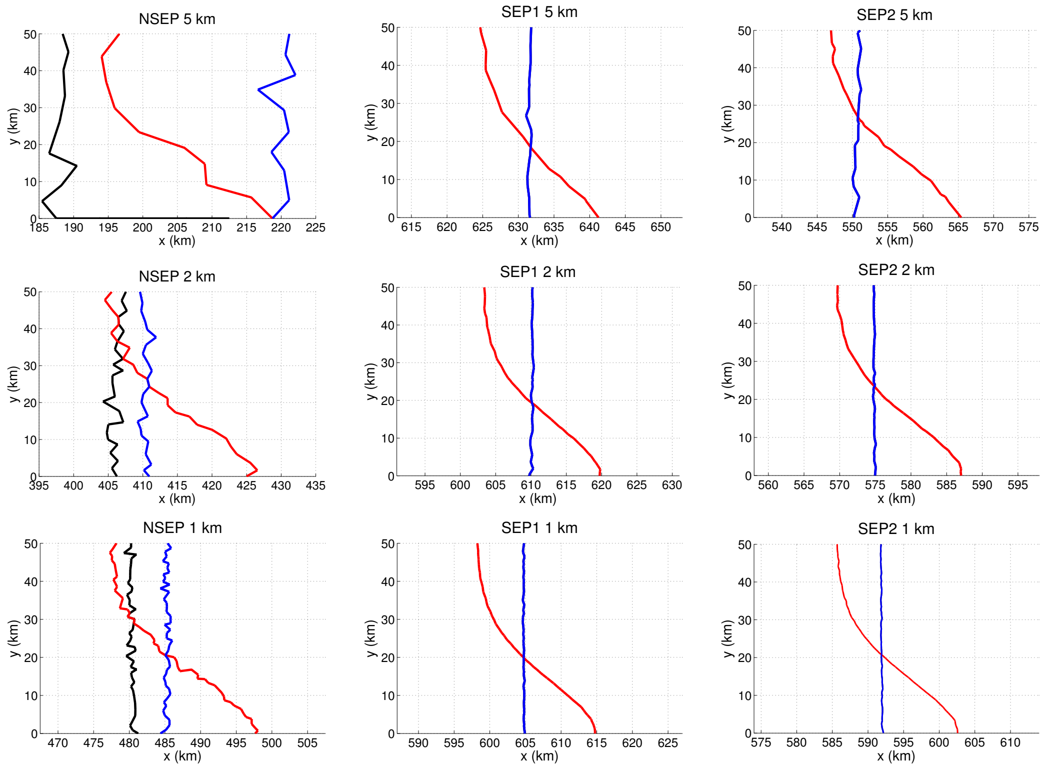

Fig. 3. ~~Steady~~ Initial steady state grounding line ~~position~~ positions in the (x,y) plane ~~before~~ (black line), ~~after (blue) the friction perturbation and~~ position 100 years ~~into~~ after the basal perturbation is introduced (red line) ~~plane for coarse mesh resolutions~~and new steady state position after the basal friction is reset to its initial value (blue line). Where black line is not visible, black and blue lines superimpose. x and y axis have the same scale for all plots.

results of this experiment: the

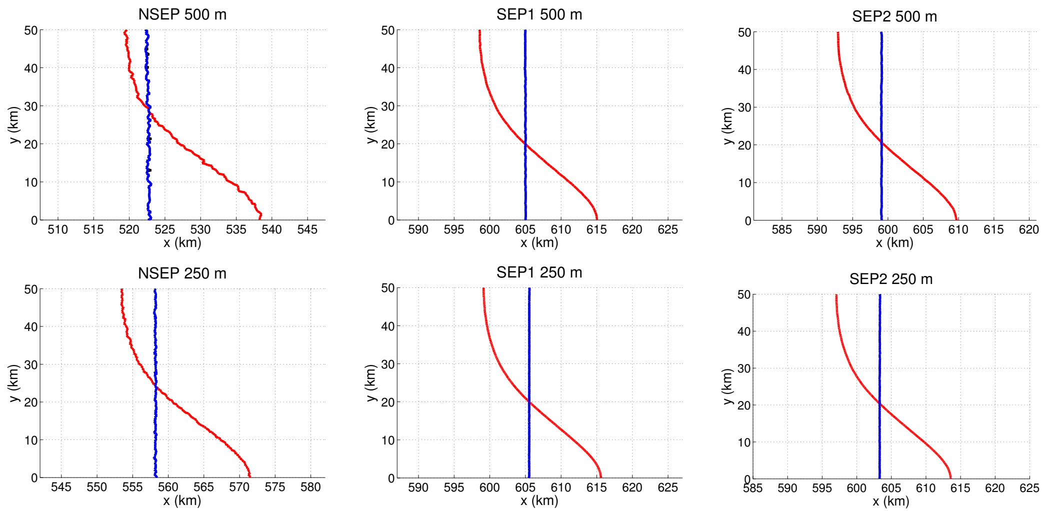

Fig. 4. ~~Steady~~ Initial steady state grounding line ~~position~~ positions in the (x,y) plane ~~before~~ (black line), ~~after (blue) the friction perturbation and~~ position 100 years ~~into~~ after the basal perturbation is introduced (red line) ~~plane for coarse mesh resolutions~~and new steady state position after the basal friction is reset to its initial value (blue line). Where black line is not visible, black and blue lines superimpose. x and y axis have the same scale for all plots.

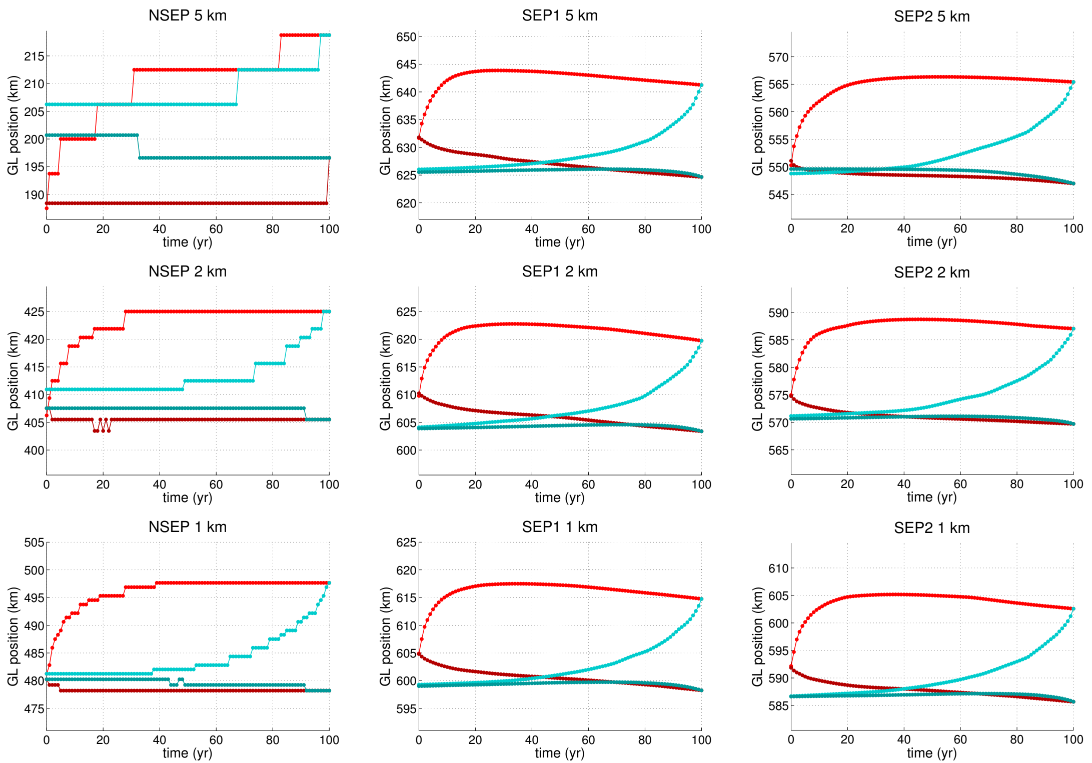

Fig. 5. Time-dependent position of the grounding line along the symmetry axis ($y = 0$) and the free slip border ($y = 50$) during (respectively light red and dark red) and after (respectively light ~~green~~ teal and dark ~~green~~teal) the friction perturbation for coarse mesh resolutions. y axes have the same scale for all simulations. x axes (time) is after the perturbation experiment (teal lines)

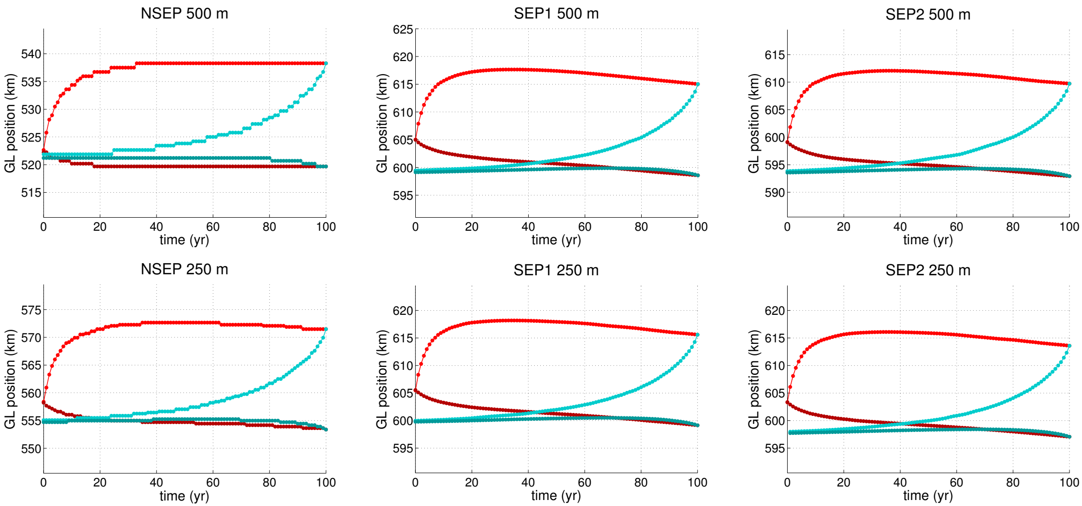

Fig. 6. Time-dependent position of the grounding line along the symmetry axis ($y = 0$) and the free slip border ($y = 50$) during (respectively light red and dark red) and after (respectively light ~~green~~ teal and dark ~~green~~teal) the friction perturbation for coarse mesh resolutions. y axes have the same scale for all simulations. x axes (time) is after the perturbation experiment (teal lines)

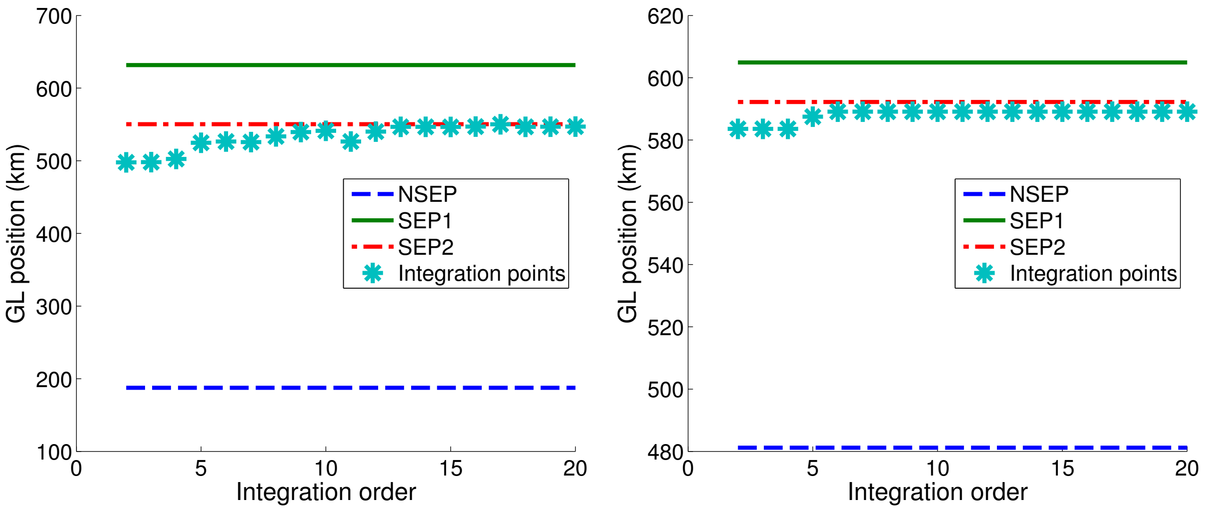

Fig. 7. Grounding line position in $y = 0$ for 5 km (left) and 1 km (right) resolution mesh for NSEP (dark blue dashed line), SEP1 (green straight line), SEP2 (red dash dotted line) and SEP3 with different integration orders (light blue stars).

Table 2. Grounding line displacement during the perturbation experiment for the ~~fifteen models~~15 simulations.

GL Parameterization	Resolution	ΔGL($y = 0$ km)	ΔGL($y = 50$ km)
NSEP	5 km	31.3 km	-12.5 km
NSEP	2 km	18.8 km	-2.1 km
NSEP	1 km	18.7 km	-2.0 km
NSEP	500 m	15.6 km	-2.6 km
NSEP	250 m	13.1 km	-4.8 km
SEP1	5 km	9.6 km	-7.1 km
SEP1	2 km	10.0 km	-6.9 km
SEP1	1 km	9.8 km	-6.5 km
SEP1	500 m	10.0 km	-6.4 km
SEP1	250 m	10.1 km	-6.4 km
SEP2	5 km	15.1 km	-4.1 km
SEP2	2 km	12.1 km	-5.0 km
SEP2	1 km	10.4 km	-6.1 km
SEP2	500 m	10.6 km	-6.2 km
SEP2	250 m	10.4 km	-6.3 km

References

Blatter, H.: Velocity And Stress-Fields In Grounded Glaciers: A Simple Algorithm For Including Deviatoric Stress Gradients, J. Glaciol., 41, 333–344, 1995.

Bohlander, J. and Scambos, T.: Antarctic coastlines and grounding line derived from MODIS Mosaic of Antarctica (MOA), digital media, Natl. Snow and Ice Data Cent., Boulder, 2007.

Cornford, S., Martin, D., Graves, D., Ranken, D. F., Le Brocq, A. M., Gladstone, R., Payne, A., Ng, E., and Lipscomb, W.: Adaptive mesh, finite volume modeling of marine ice sheets, J. Comput. Phys., 232, 529–549, doi:10.1016/j.jcp.2012.08.037, 2013.

Courant, R., Friedric.K, and Lewy, H.: On Partial Difference Equations Of Mathematical Physics, Ibm Journal Of Research And Development, 11, 215–234, 1967.

Cuffey, K. and Paterson, W. S. B.: The Physics of Glaciers, 4th Edition, Elsevier, Oxford, 2010.

Durand, G., Gagliardini, O., de Fleurian, B., Zwinger, T., and Le Meur, E.: Marine ice sheet dynamics: Hysteresis and neutral equilibrium, J. Geophys. Res., 114, 1–10, doi:10.1029/2008JF001170, 2009a.

Durand, G., Gagliardini, O., Zwinger, T., Le Meur, E., and Hindmarsh, R.: Full Stokes modeling of marine ice sheets: influence of the grid size, Ann. Glaciol., 50, 109–114, 2009b.

Favier, L., Durand, G., Cornford, S. L., Gudmundsson, G. H., Gagliardini, O., Gillet-Chaulet, F., Zwinger, T., Payne, A. J., and Le Brocq, A.: Retreat of Pine Island Glacier controlled by marine ice-sheet instability, Nat. Clim. Change, pp. 1–5, doi:DOI:10.1038/NCLIMATE2094, 2014.

Feldmann, J., Albrecht, T., Khroulev, C., F., P., and Levermann, A.: Resolution-dependent performance of grounding line motion in a shallow model compared with a full-Stokes model according to the MISMIP3d intercomparison, J. Glaciol., 60, 353–359, doi:10.3189/2014JoG13J093, 2014.

Gladstone, R. M., Lee, V., Vieli, A., and Payne, A. J.: Grounding line migration in an adaptive mesh ice sheet model, J. Geophys. Res., 115, 1–19, doi:10.1029/2009JF001615, 2010a.

Gladstone, R. M., Payne, A. J., and Cornford, S. L.: Parameterising the grounding line in flow-line ice sheet models, The Cryosphere, 4, 605–619, doi:10.5194/tc-4-605-2010, http://www.the-cryosphere.net/4/605/2010/, 2010b.

Goldberg, D., Holland, D. M., and Schoof, C.: Grounding line movement and ice shelf buttressing in marine ice sheets, J. Geophys. Res., 114, 1–23, doi:10.1029/2008JF001227, 2009.

Goldstein, R., Engelhardt, H., Kamb, B., and Frolich, R.: Satellite Radar Interferometry for Monitoring ice-sheet motion: Application to an antarctic ice stream, Science, 262, 1525–1530, 1993.

Gudmundsson, G.: Analytical solutions for the surface response to small amplitude perturbations in boundary data in the shallow-ice-stream approximation, The Cryosphere, 2, 77–93, 2008.

Hindmarsh, R.: A numerical comparison of approximations to the Stokes equations used in ice sheet and glacier modeling, J. Geophys. Res., 109, 1–15, doi:10.1029/2003JF000065, 2004.

Hindmarsh, R. and Le Meur, E.: Dynamical processes involved in the retreat of marine ice sheets, J. Glaciol., 47, 271–282, 2001.

Huybrechts, P.: A 3-D model for the Antarctic ice sheet: a sensitivity study on the glacial-interglacial contrast, Clim. Dyn., 5, 79–92, 1990.

Katz, R. F. and Worster, M.: Stability of ice-sheet grounding lines, Proc. R. Soc. A, 466, 15971620, doi:10.1098/rspa.2009.0434, 2010.

Larour, E., Seroussi, H., Morlighem, M., and Rignot, E.: Continental scale, high order, high spatial resolution, ice sheet modeling using the Ice Sheet System Model (ISSM), J. Geophys. Res., 117, 1–20, doi:10.1029/2011JF002140, 2012.

MacAyeal, D.: Large-scale ice flow over a viscous basal sediment: Theory and application to Ice Stream B, Antarctica, J. Geophys. Res., 94, 4071–4087, 1989.

Morlighem, M., Rignot, E., Seroussi, H., Larour, E., Ben Dhia, H., and Aubry, D.: Spatial patterns of basal drag inferred using control methods from a full-Stokes and simpler models for Pine Island Glacier, West Antarctica, Geophys. Res. Lett., 37, 1–6, doi:10.1029/2010GL043853, 2010.

Nowicki, S. M. J. and Wingham, D. J.: Conditions for a steady ice sheet-ice shelf junction, Earth Planet. Sci. Lett., 265, 246–255, 2008.

Pattyn, F.: A new three-dimensional higher-order thermomechanical ice sheet model: Basic sensitivity, ice stream development, and ice flow across subglacial lakes, J. Geophys. Res., 108, 1–15, doi:10.1029/2002JB002329, 2003.

Pattyn, F. and Durand, G.: Why marine ice sheet model predictions may diverge in estimating future sea level rise, Geophys. Res. Lett., 40, 4316–4320, doi:10.1002/grl.50824, http://onlinelibrary.wiley.com/doi/10.1002/grl.50824/abstract, 2013.

Pattyn, F., Huyghe, A., De Brabander, S., and De Smedt, B.: Role of transition zones in marine ice sheet dynamics, J. Geophys. Res. - Earth Surface, 111, 1–10, doi:10.1029/2005JF000394, 2006.

Pattyn, F., Schoof, C., Perichon, L., Hindmarsh, R. C. A., Bueler, E., de Fleurian, B., Durand, G., Gagliardini, O., Gladstone, R., Goldberg, D., Gudmundsson, G. H., Huybrechts, P., Lee, V., Nick, F. M., Payne, A. J., Pollard, D., Rybak, O., Saito, F., and Vieli, A.: Results of the Marine Ice Sheet Model Intercomparison Project, MISMIP, The Cryosphere, 6, 573–588, doi:10.5194/tc-6-573-2012, 2012.

Pattyn, F., Perichon, L., Durand, G.and Favier, L., Gagliardini, O., Hindmarsh, R. C. A., Zwinger, T., Albrecht, T., Cornford, S., Docquier, D., Fuerst, J., Goldberg, D., Gudmundsson, H., Humbert, A., Hutten, M., Huybrecht, P., Jouvet, G., Kleiner, T., Larour, E., Martin, D., Morlighem, M., Payne, A., Pollard, D., Ruckamp, M., Rybak, O., Seroussi, H., Thoma, M., and Wilkens, N.: Grounding-line migration in plan-view marine ice-sheet models: results of the ice2sea MISMIP3d intercomparison, J. Glaciol., 59 (215), 410–422, doi:10.3189/2013JoG12J129, 2013.

Raymond, C.: Shear margins in glaciers and ice sheets, J. Glaciol., 42, 90–102, 1996.

Rignot, E., Mouginot, J., and Scheuchl, B.: Antarctic grounding line mapping from differential satellite radar interferometry, Geophys. Res. Lett., 38, 1–6, doi:10.1029/2011GL047109, 2011a.

Rignot, E., Velicogna, I., van den Broeke, M., Monaghan, A., and Lenaerts, J.: Acceleration of the contribution of the Greenland and Antarctic ice sheets to sea level rise, Geophys. Res. Lett., 38, 1–5, doi:10.1029/2011GL046583, 2011b.

Ritz, C., Rommelaere, V., and Dumas, C.: Modeling the evolution of Antarctic ice sheet over the last 420,000 years: Implications for altitude changes in the Vostok region, J. Geophys. Res., 106, 31 943–31 964, doi:10.1029/2001JD900232, http://www.agu.org/pubs/crossref/2001/2001JD900232.shtml, 2001.

Schodlok, M., Menemenlis, D., Rignot, E., and Studinger, M.: Sensitivity of the ice-shelf/ocean system to the sub-ice-shelf cavity shape measured by NASA IceBridge in Pine Island Glacier, West Antarctica, Ann. Glaciol., 53(60), 156–162, doi:10.3189/2012AoG60A073, 2012.

Schoof, C.: Marine ice-sheet dynamics. Part 1. The case of rapid sliding, J. Fluid Mech., 573, 27–55, doi:10.1017/S0022112006003570, 2007a.

Schoof, C.: Ice sheet grounding line dynamics: Steady states, stability, and hysteresis, J. Geophys. Res., 112, 1–19, doi:10.1029/2006JF000664, 2007b.

van der Veen, C.: Response of a Marine Ice-Sheet to Changes at the Grounding Line, Quaternary Research, 24, 257–267, doi:10.1016/0033-5894(85)90049-3, 1985.

Vieli, A. and Payne, A.: Assessing the ability of numerical ice sheet models to simulate grounding line migration, J. Geophys. Res., 110, 1–18, doi:10.1029/2004JF000202, 2005.

Weertman, J.: Stability of the junction of an ice sheet and an ice shelf, J. Glaciol., 13(67), 3–11, 1974.

Winkelmann, R., Martin, M. A., Haseloff, M., Albrecht, T., Bueler, E., Khroulev, C., and Levermann, A.: The Potsdam Parallel Ice Sheet Model (PISM-PIK) - Part 1: Model description, The Cryosphere, 5, 715–726, doi:10.5194/tc-5-715-2011, 2011.

Zienkiewicz, O. C. and Taylor, R. L.: The finite element method, vol. 1, New York, London, fourth edn., 1989.